Expanded View Figures

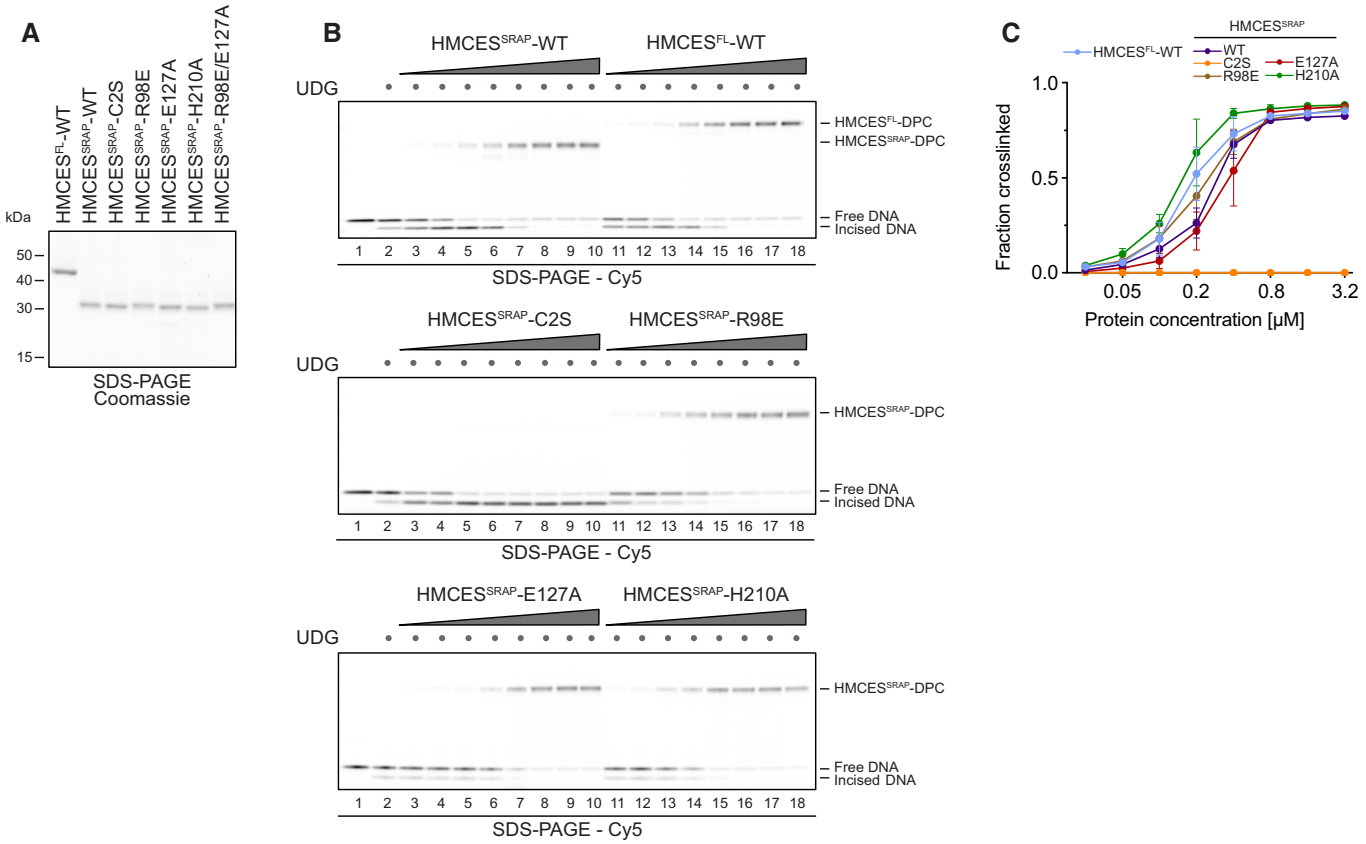

Figure EV1. HMCES-DNA-protein crosslinks are reversible. Related to Fig 1.

A Coomassie-stained SDS–PAGE gel showing recombinant purified human HMCES^{FL}-WT, HMCES^{SRAP}-WT, HMCES^{SRAP}-C2S, HMCES^{SRAP}-R98E, HMCES^{SRAP}-E127A, HMCES^{SRAP}-H210A and HMCES^{SRAP}-R98E/E127A proteins used in this study.

B DPC formation of HMCES^{FL} and HMCES^{SRAP} (WT or indicated variants). dU-containing DNA (0.1 μM) was incubated alone or with UDG and increasing concentrations of HMCES (0.025, 0.05, 0.1, 0.2, 0.4, 0.8, 1.6 and 3.2 μM), as indicated for 1 h at 37°C prior to analysis by denaturing SDS–PAGE.

C Quantification of HMCES-DPC formation assays shown in (B).

Data information: Data in (C) represent the mean of three individual experiments ± SD.

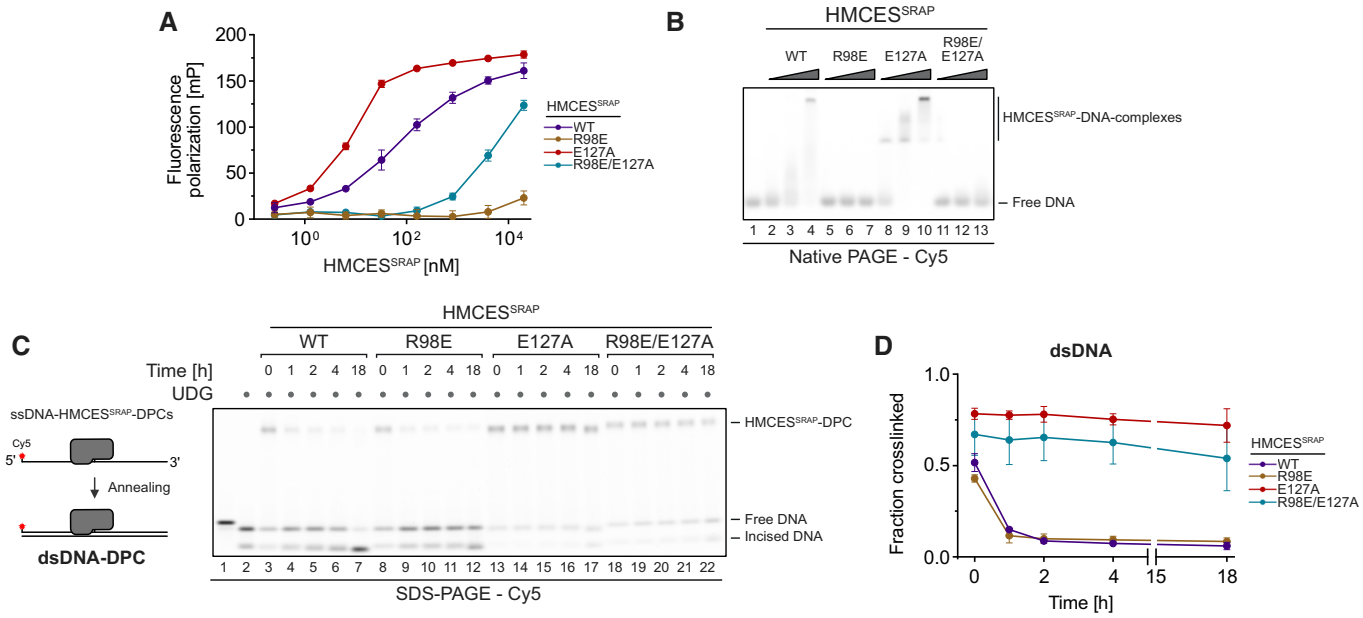

Figure EV2. Release of HMCES-DPCs is determined by DNA context. Related to Fig 3.

A Fluorescence polarization measurements of Cy5-labelled ssDNA (25 nM) incubated with increasing concentrations of HMCES^{SRAP}-WT, HMCES^{SRAP}-R98E, HMCES^{SRAP}-E127A or HMCES^{SRAP}-R98E/E127A for 20 min on ice prior to measuring fluorescence polarization.

B Non-covalent DNA binding of indicated HMCES^{SRAP} variants was assessed by electrophoretic mobility shift assay. A Cy5-labelled 30-mer ssDNA (0.1 μM) was incubated with HMCES^{SRAP} (0, 0.125, 0.5 or 2 μM) for 20 min at 4°C prior to analysis by native PAGE.

C DPC reversal kinetics of indicated HMCES^{SRAP} variants in dsDNA. A corresponding reverse oligonucleotide was annealed to HMCES^{SRAP}-DPCs, before incubation for the indicated amount of time at 37°C prior to separation by denaturing SDS–PAGE.

D Quantification of DPC reversal assays shown in (C).

Data information: Data in (A) and (D) represent the mean of three independent experiments ± SD.

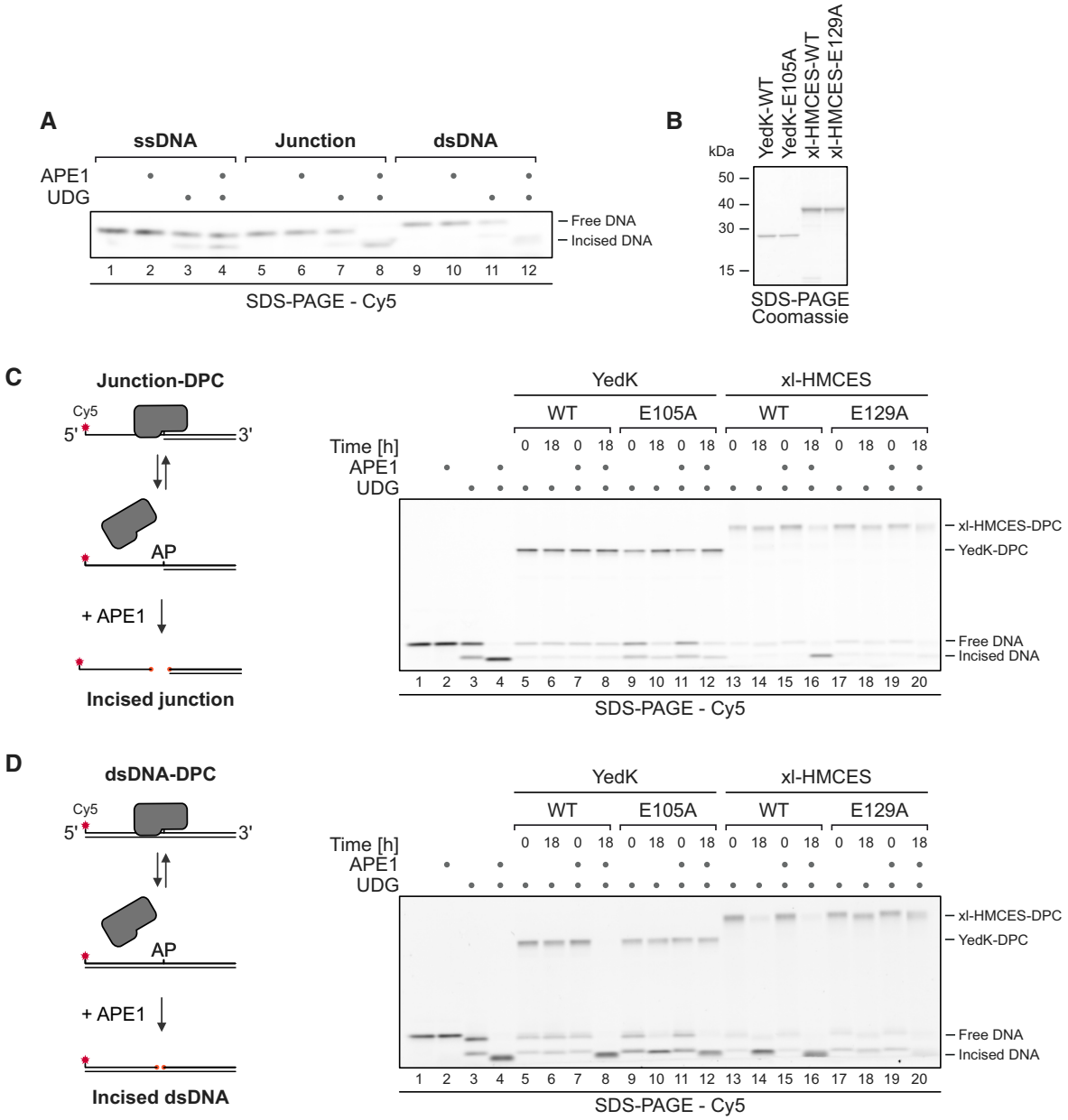

Figure EV3. Auto-release of HMCES-DPCs restricts crosslink formation to physiologically relevant situations. Related to Fig 5.

A APE1 incision of an AP site in ssDNA, DNA junction and dsDNA. A Cy5-labelled 30-mer ssDNA was incubated alone or with UDG for 1 h at 37°C. Corresponding reverse oligonucleotides for DNA junction or dsDNA were annealed (for ssDNA, a non-complementary oligonucleotide was added). Next, samples were incubated with APE1 for 18 h at 37°C before separation by denaturing SDS–PAGE.

B Coomassie-stained SDS–PAGE gel showing recombinant purified bacterial YedK-WT, YedK-E105A, xl-HMCES-WT and xl-HMCES-E129A proteins used in this study.

C, D APE1 incision of an AP site protected by the indicated YedK-WT-DPC or YedK-E105A-DPC and xl-HMCES-WT-DPC or xl-HMCES-E129A-DPC at ssDNA-dsDNA junctions (C) or within dsDNA (D). Free dU-containing DNA was incubated alone or in the presence of UDG and YedK/xl-HMCES for 1 h at 37°C. Next, corresponding reverse oligonucleotides were annealed to generate an ssDNA-dsDNA junction (C) or dsDNA (D), and reactions were incubated alone or with APE1 for the indicated amount of time at 37°C prior to separation by denaturing SDS–PAGE.

Figure EV4. Resolution of HMCES-DPCs during replication-coupled ICL repair. Related to Fig 5.

A Schematic depiction of the NEIL3-dependent repair of an AP-ICL, a lesion that forms when an AP site reacts with a nucleobase of the opposing DNA strand forming a covalent crosslink (Price *et al*, 2014). In *Xenopus* egg extracts, such crosslinks are primarily unhooked by the NEIL3 glycosylase (Semlow *et al*, 2016), which yields an AP site leading to formation of an HMCES-DPC.

B–F In the absence of SPRTN, the intact HMCES-DPC is presumably bypassed by TLS and transferred into dsDNA. To test whether this triggers autorelease, we analysed the stability of DPCs formed by wild-type and E129A-mutated *Xenopus laevis* rHMCES-3xFlag proteins during ICL repair in egg extract. pICL-*lacO*^{AP} was replicated in mock- or SPRTN-depleted extracts (B) supplemented with WT or E129A rHMCES-3xFlag. At the time points indicated, plasmid was recovered under stringent conditions, the DNA was digested and released proteins were separated by SDS–PAGE. HMCES-DPCs were detected using an antibody raised against the SRAP domain that permits simultaneous monitoring of endogenous HMCES protein and the recombinant 3xFlag-tagged HMCES (which migrates slower during SDS–PAGE due to the 3xFlag). In this experimental setup, the endogenous protein serves as a control for the effects of SPRTN depletion and autorelease. Like the endogenous HMCES (C), both WT (D) and E129A-mutated rHMCES-3xFlag (E) were stabilized by SPRTN depletion, implying that proteolysis is the dominant mechanism for removing HMCES-DPC under these conditions. However, it was challenging to assess the relative behaviour of tagged WT and mutant protein because DPCs formed by the wild-type recombinant protein (like those formed by the endogenous protein) are resolved slowly in SPRTN-depleted extract (on the timescale of hours, somewhat slower than the timescale for observed for reversal *in vitro*). Additionally, the E129A-mutated recombinant flag-tagged protein crosslinked less efficiently than endogenous HMCES, making it difficult to detect even when present in large excess (F). We are, therefore, unable to determine from these data whether HMCES-DPC reversal occurs during ICL repair in egg extract under the conditions tested. Orange dots denote non-specific bands or bands corresponding to contaminating IgG.

G One explanation for the discrepancy in the degree of reversal observed between the *in vitro* reconstitution and egg extract systems could be that the *in vitro* reactions were all performed at 37°C, while replication in egg extracts must be performed at 20°C. Therefore, we assessed reversal of HMCES^{SRAP}-WT or -E127A-DPCs in dsDNA at the indicated temperatures for the indicated amount of time before analysis by denaturing SDS–PAGE. Indeed, autocatalytic reversal was significantly delayed at 20°C.

H Quantification of DPC reversal assays using HMCES^{SRAP}-WT and -E127A shown in (G).

I The extracts used in the replication reactions shown in (J and K) were immunoblotted for SPRTN, Rev1 and HMCES.

J As an alternative additional strategy to determine whether reversal contributes to HMCES-DPC resolution, we tested whether REV1 depletion results in stabilization of HMCES-DPCs, reasoning that blocking TLS (and transfer of the DPC into dsDNA) may inhibit reversal. pICL-*lacO*^{AP} was replicated in mock-, REV1-, SPRTN- or REV1- and SPRTN-depleted egg extracts, as indicated. At the indicated time points, plasmid was recovered under stringent conditions, the DNA was digested and released proteins were separated by SDS–PAGE. HMCES was detected by blotting. As expected, depletion of SPRTN alone resulted in a strong stabilization of HMCES-DPCs. Depletion of REV1 alone did not stabilize HMCES-DPCs, consistent with our data indicating that SPRTN represents the dominant mechanism for HMCES-DPC resolution in egg extract. Surprisingly, when combined with SPRTN depletion, REV1 depletion partially suppressed the accumulation of HMCES-DPCs. Superficially, this result is contrary to our expectations based on data presented in Fig 6. However, we interpret the result to indicate when the HMCES-DPC is maintained at an ssDNA/dsDNA junction due to inefficient TLS, residual SPRTN or another protease can eventually degrade the HMCES-DPC. Therefore, while these data do not provide evidence for HMCES-DPC reversal during ICL repair in egg extract, they do reinforce the need for alternative removal mechanisms for HMCES-DPCs present in dsDNA that are refractory to proteolysis.

K In parallel with the reactions shown in (J), pICL-*lacO*^{AP} was replicated in the indicated egg extracts supplemented with [α-^{32}P]dCTP. Replication intermediates were separated on a native agarose gel and visualized by autoradiography. SC, supercoiled. OC, open circular. Consistent with a TLS defect upon Rev1 depletion, we observed accumulation of gapped, circular plasmids in replication gels, implying that the HMCES-DPC is maintained at an ssDNA-dsDNA junction.

Data information: Data in (H) represent the mean of three independent experiments ± SD.

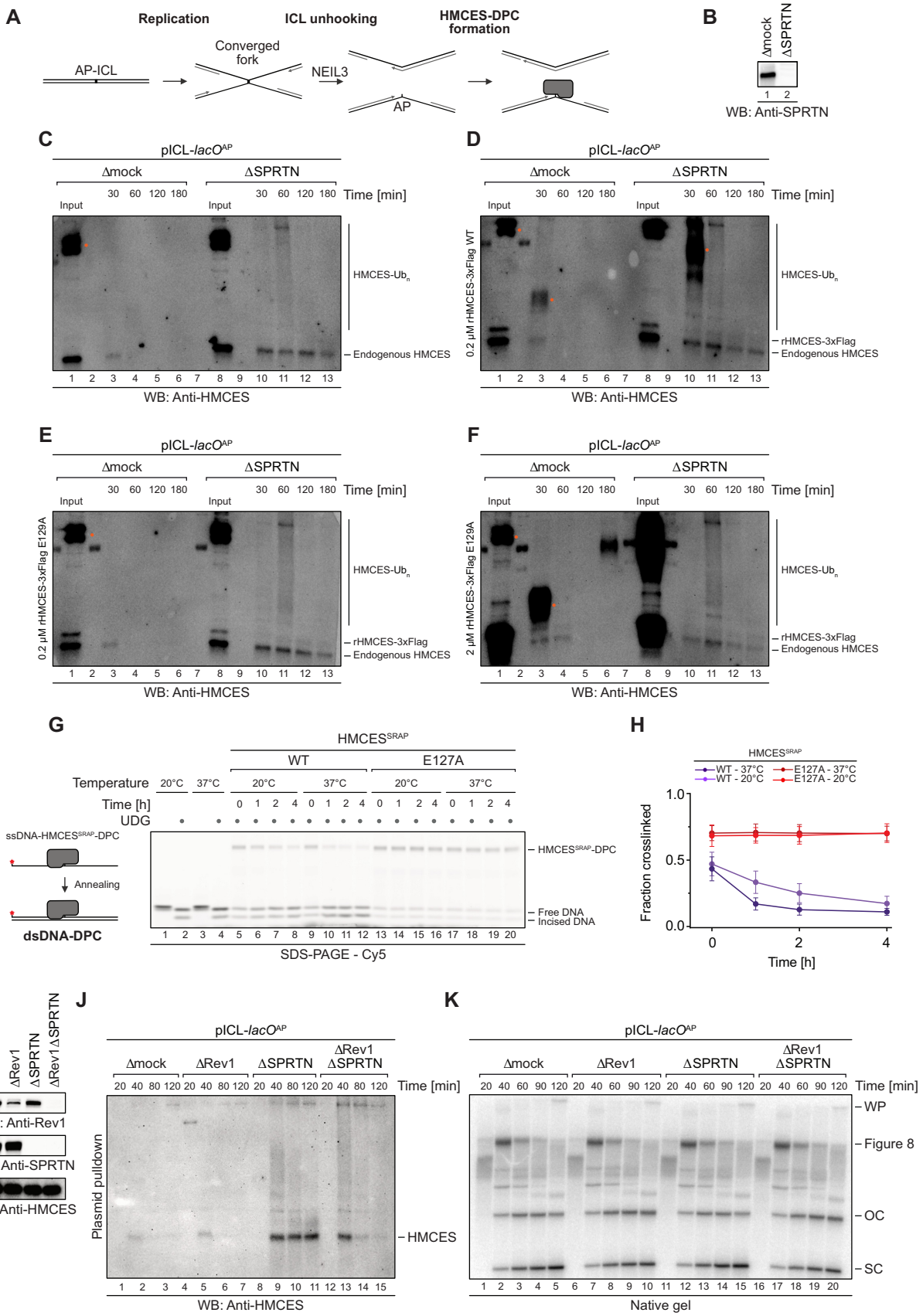

Figure EV4.

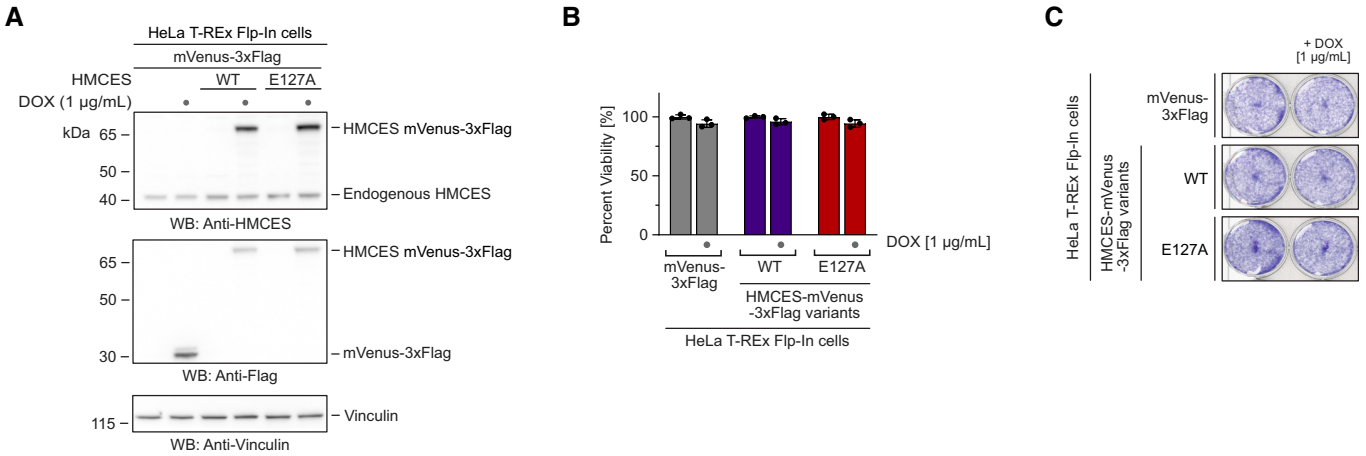

Figure EV5. Cell viability is not affected upon overexpression of reversal-defective HMCES variants. Related to Fig 7.

A–C HeLa T-REx Flp-In cells expressing the indicated doxycycline-inducible HMCES variants with a C-terminal mVenus-3xFlag-tag were grown in the presence of 1 µg/ml doxycycline, as indicated. Expression levels were analysed by Western blotting (A). Cell viability was determined using AlamarBlue cell viability assay (B), or crystal violet staining (C).

Data information: Data in (B) represent the mean ± SD of three technical replicates normalized to the mean of untreated control (mVenus-DOX).